

Impact of Kuchowicz Metric Function on Gravastars in $f(R, T)$ Theory

M. Sharif ^{*} and Arfa Waseem [†]

Department of Mathematics, University of the Punjab,
Quaid-e-Azam Campus, Lahore-54590, Pakistan.

Abstract

This paper discusses the configuration of gravitational vacuum star or gravastar with the impact of geometry and matter coupling present in $f(R, T)$ gravity. The gravastar is also conceptualized as a substitute for a black hole which is illustrated by three geometries known as (1) the interior geometry, (2) the intermediate thin-shell and (3) the exterior geometry. For a particular $f(R, T)$ model, we analyze these geometries corresponding to Kuchowicz metric function. We evaluate another metric potential for the interior domain as well as the intermediate shell which is non-singular for both domains. The Schwarzschild metric is adopted to demonstrate the exterior geometry of gravastar, while the numerical values of unknown constants are calculated through boundary conditions. Finally, we discuss different features of gravastar regions like proper length, energy, surface redshift as well as equation of state parameter. We conclude that the gravastar model can be regarded as a successful replacement of the black hole in the context of this gravity.

Keywords: Gravastar; $f(R, T)$ gravity; Kuchowicz metric function.

PACS: 04.40.Dg; 04.50.Kd.

^{*}msharif.math@pu.edu.pk

[†]arfawaseem.pu@gmail.com

1 Introduction

There exist enormous astrophysical phenomena including gravitational collapse as well as stellar evolution that have become the center of attention for many researchers. Stellar evolution describes a process that manifests the entire life cycle of a self-gravitating object whereas the phenomenon of gravitational collapse is the cause behind the production of new and massive compact celestial bodies like neutron stars, white dwarfs and black holes. The last result of this collapsing phenomenon is entirely based upon the parent masses of stellar objects. Recently, several researchers have proposed that densest objects other than black holes can be created as the outcome of massive collapsing stars. In this regard, Mazur and Mottola [1] developed an elegant model of an extremely compact object named as gravitational vacuum star or in short gravastar. Gravastar is identified as the non-singular extremely compact spherically symmetric candidate that may be considered as compact as the classical black hole.

According to this model, the geometry of gravastar is demonstrated by three different regions where the interior geometry depends upon the de Sitter core with an equation of state (EoS) $\rho = -p > 0$, surrounded by a thin-shell with stiff matter and the external vacuum domain is expressed by the Schwarzschild spacetime. The notion of gravastar geometries is significantly attractive for the astrophysicists as it may resolve the fundamental issues associated with black holes, i.e., the information paradox and the issue of singularity. It is believed that a phase transition occurs in the interior of gravastar that generates a de Sitter core with repulsive effects which assist to balance the collapsing body and prevent the generation of singularity [2]. This transition appears very close to the bound $\frac{2m}{r} = 1$ which makes difficult for an observer to differentiate the gravastar from a black hole.

Despite several theoretical and observational achievements, there are still complicated issues that motivate the researchers to explore different substitutes in which the collapsing results are very large stars without event horizons [2]-[4]. Among those giant stars, gravastars have inspired the astrophysicists to explore their geometries using various techniques. In general relativity (GR), Visser and Wiltshire [5] examined the stability of gravastars and observed that different EoS provide the dynamically stable distribution of gravastars. Carter [6] established new exact solutions of gravastars and found different effects of EoS on the exterior and interior regions. Bilić et al. [7] investigated the core solutions of gravastars by inducing the Born-Infeld

phantom in place of de Sitter metric and examined that at the center of galaxies, their results can illustrate the dark compact structures.

Horvat and Ilijić [8] analyzed the behavior of energy bounds within the gravastar shell and discussed the stability through radial oscillations and sound speed on the shell. Many researchers [9]-[14] presented exact interior solutions of gravastar by employing various EoS corresponding to different conjectures. Lobo and Arellano [15] formulated distinct models of gravastars under the impact of nonlinear electrodynamics and inspected some particular characteristics of their models. Horvat et al. [16] generalized the notion of gravastar by inserting the effects of electric field and derived the surface redshift, EoS parameter as well as stability for the inner and outer geometries. In the same scenario, Turimov et al. [17] examined the magnetic field configuration and obtained exact solutions corresponding to the interior geometry of a slowly rotating gravastar.

In cosmological scenarios, the mysteries of dark constituents, responsible for the expanding cosmos, lead to the formation of extended or modified gravitational theories to GR. The concept of coupling between matter and curvature yields several modified theories like $f(R, T)$ gravity [18], $f(R, T, R_{\gamma\eta}T^{\gamma\eta})$ theory [19] and $f(\mathcal{G}, T)$ gravity [20], where R indicates the curvature invariant, T reveals the trace of energy-momentum tensor (EMT) and \mathcal{G} symbolizes the Gauss-Bonnet invariant. In these theories, $f(R, T)$ theory has attained much importance in describing various astrophysical objects corresponding to different approaches [21]-[28]. The study of gravastar has motivated the researchers to discuss the effects of modified theories on structural properties of gravastar. In $f(R, T)$ framework, Das et al. [29] analyzed the speculation of gravastar and studied its features graphically with respect to different EoS. Shamir and Ahmad [30] exhibited singularity free solutions of gravastar and extracted mathematical forms of several physical quantities in $f(\mathcal{G}, T)$ background.

The physical viability as well as stability of gravastar models have also been analyzed with the impact of anisotropic pressure configuration. Cattoen et al. [31] expressed the extended form of gravastar that comprises anisotropic pressure component beyond the presence of thin-shell. They observed that pressure anisotropy is the most fundamental ingredient for all gravastar like objects. DeBenedictis et al. [32] obtained anisotropic interior solutions of gravastar by considering different density functions and EoS. Chan et al. [33] analyzed energy conditions of gravastars corresponding to anisotropic dark energy as well as phantom energy fluid distribution. They

found that isotropic/anisotropic interior matter configuration can perturb the creation of gravastar and the production is feasible when the radial pressure is less than the tangential pressure.

In the analysis of stellar compact structures, the solutions of the field equations play a significant role. Ghosh et al. [34] presented the structure of gravastar by considering the Kuchowicz metric function in GR. They displayed the graphical behavior of various features and found stable structure of gravastar under the influence of their considered singularity free metric function. We have inspected the effects of electric field on the structure of gravastar in $f(R, T)$ framework by adopting the conformal Killing vectors [35]. Ghosh with his collaborators [36] determined a unique solution of gravastar through embedding class 1 technique by implementing the Karmarkar condition. They obtained exact solutions of the intermediate shell and evaluated non-singular finite solutions for the inner domain of gravastar.

In this paper, we evaluate singularity free solutions of gravastar admitting the Kuchowicz metric function in $f(R, T)$ gravity. We determine another metric function for the intermediate shell as well as interior geometry of gravastar. We present the graphical variations of different features of gravastar shell for specific $f(R, T)$ model. We adopt the following pattern for the presentation of this paper. Next section displays the fundamental formulation of this theory. Section 3 expresses three geometries of gravastar with Kuchowicz metric function. The graphical description of obtained solutions corresponding to the calculated values of unknown constants and model parameter is presented in section 4. The last section provides the concluding remarks.

2 Fundamentals of $f(R, T)$ Theory

The modified action for $f(R, T)$ gravity coupled with Lagrangian matter density (L_M) is characterized by [18]

$$\mathcal{A}_{f(R,T)} = \int \sqrt{-g} \left[\frac{f(R, T)}{2\kappa} + L_M \right] d^4x, \quad (1)$$

in which g exhibits the determinant of $g_{\gamma\eta}$ and $\kappa = \frac{8\pi G}{c^4}$ denotes the coupling constant with speed of light ($c = 1$) and gravitational constant ($G = 1$). The

$f(R, T)$ field equations are

$$\begin{aligned} f_R(R, T)R_{\gamma\eta} &= \frac{g_{\gamma\eta}f(R, T)}{2} - (\nabla_\gamma\nabla_\eta - g_{\gamma\eta}\square)f_R(R, T) \\ &= 8\pi T_{\gamma\eta} - (T_{\gamma\eta} + \Theta_{\gamma\eta})f_T(R, T), \end{aligned} \quad (2)$$

with ∇_γ symbolizes the covariant differentiation, $f_R(R, T) = [f(R, T)]_{,R}$, $f_T(R, T) = [f(R, T)]_{,T}$, $\square = g^{\gamma\eta}\nabla_\gamma\nabla_\eta$ and $\Theta_{\gamma\eta}$ is specified by

$$\Theta_{\gamma\eta} = g^{\beta\nu}\frac{\delta T_{\beta\nu}}{\delta g^{\gamma\eta}} = g_{\gamma\eta}L_m - 2T_{\gamma\eta} - 2g^{\beta\nu}\frac{\partial^2 L_m}{\partial g^{\gamma\eta}\partial g^{\beta\nu}}. \quad (3)$$

The covariant derivative of Eq.(2) yields

$$\nabla^\gamma T_{\gamma\eta} = \frac{f_T}{8\pi - f_T} \left[(T_{\gamma\eta} + \Theta_{\gamma\eta})\nabla^\gamma(\ln f_T) - \frac{g_{\gamma\eta}}{2}\nabla^\gamma T + \nabla^\gamma\Theta_{\gamma\eta} \right]. \quad (4)$$

This expression demonstrates that the conservation law in curvature-matter coupled theories is not executed by the EMT.

To explore the astrophysical structures, the configuration of matter shows a significant effect. The non-zero elements of EMT manifest the dynamical constituents possessing distinct physical significance. To study the features of gravastars, we assume perfect matter configuration as

$$T_{\gamma\eta} = (p + \rho)\mathcal{U}_\gamma\mathcal{U}_\eta - pg_{\gamma\eta}. \quad (5)$$

Here, ρ symbolizes the density, p indicates the pressure while \mathcal{U}_γ reveals the four velocity. For matter configuration, there exist several choices of L_m . Here, we choose $L_m = -p$ giving $\frac{\partial^2 L_m}{\partial g^{\gamma\eta}\partial g^{\mu\nu}} = 0$ and $\Theta_{\gamma\eta} = -2T_{\gamma\eta} - pg_{\gamma\eta}$ [18]. We consider a linear $f(R, T)$ model in which matter and geometric components are minimally coupled as

$$f(R, T) = R + 2h(T), \quad (6)$$

where $h(T)$ indicates the arbitrary function of the trace of EMT. In order to obtain the EMT for modified gravitational theory, we suppose $h(T) = \alpha T$ where α acts as a coupling constant and $T = \rho - 3p$. The corresponding linear form of $f(R, T)$ becomes

$$f(R, T) = R + 2\alpha T. \quad (7)$$

Here, the induction of T yields the more extended form of GR as compared to $f(R)$ theory. This form was firstly suggested by Harko et al. [18] and has widely been implemented to explore the structural properties of self-gravitating bodies. Das et al. [29] adopted this functional form to evaluate exact singularity free solutions of collapsing body and explored various physically viable properties of gravastar. We have used this model to discuss the features of charged gravastars with conformal Killing vectors [35]. Insertion of this form in Eq.(2) provides

$$G_{\gamma\eta} = 8\pi T_{\gamma\eta} + \alpha T g_{\gamma\eta} + 2\alpha(T_{\gamma\eta} + p g_{\gamma\eta}), \quad (8)$$

where $G_{\gamma\eta}$ exhibits the Einstein tensor. Equation (4) for $R + 2\alpha T$ model takes the form

$$\nabla^\gamma T_{\gamma\eta} = \frac{-\alpha}{2(4\pi + \alpha)} [g_{\gamma\eta} \nabla^\gamma T + 2\nabla^\gamma (p g_{\gamma\eta})]. \quad (9)$$

For $\alpha = 0$, the usual conserved form of GR can be regained from this equation.

3 Exact Solutions in $R + 2\alpha T$ Model

The static spherically symmetric line element for the interior region is

$$ds_-^2 = e^{\chi(r)} dt^2 - e^{\xi(r)} dr^2 - r^2 d\theta^2 - r^2 \sin^2 \theta d\phi^2. \quad (10)$$

The $f(R, T)$ field equations yield

$$\frac{1}{r^2} - e^{-\xi} \left(\frac{1}{r^2} - \frac{\xi'}{r} \right) = 8\pi\rho + \alpha(3\rho - p), \quad (11)$$

$$e^{-\xi} \left(\frac{1}{r^2} + \frac{\chi'}{r} \right) - \frac{1}{r^2} = 8\pi p - \alpha(\rho - 3p), \quad (12)$$

$$e^{-\xi} \left(\frac{\chi''}{2} - \frac{\xi'}{2r} + \frac{\chi'}{2r} + \frac{\chi'^2}{4} - \frac{\chi'\xi'}{4} \right) = 8\pi p - \alpha(\rho - 3p), \quad (13)$$

where prime presents differentiation associated with radial coordinate. We consider the metric function $e^{\chi(r)}$ as Kuchowicz type [37] expressed by

$$e^{\chi(r)} = e^{Ar^2 + 2\ln B}, \quad (14)$$

where A and B are arbitrary constants. The dimension of A is $\frac{1}{L^2}$ while B is a dimensionless constant. This metric function was proposed by Kuchowicz as a non-singular function to discuss the stellar configurations. Ghosh et al. [34] employed this metric potential to analyze the features of gravastars in GR. This function provides successful theoretical assistance for massive compact objects corresponding to some particular values of arbitrary constants. Substituting Eq.(14) in (11)-(13), we have

$$\frac{1}{r^2} - e^{-\xi} \left(\frac{1}{r^2} - \frac{\xi'}{r} \right) = 8\pi\rho + \alpha(3\rho - p), \quad (15)$$

$$e^{-\xi} \left(\frac{1}{r^2} + 2A \right) - \frac{1}{r^2} = 8\pi p - \alpha(\rho - 3p), \quad (16)$$

$$e^{-\xi} \left(2A - \frac{\xi'}{2r} + A^2 r^2 - \frac{Ar\xi'}{2} \right) = 8\pi p - \alpha(\rho - 3p). \quad (17)$$

The modified conservation equation turns out to be

$$p' + Ar(p + \rho) - \frac{\alpha}{2(\alpha + 4\pi)} (\rho' - p') = 0. \quad (18)$$

3.1 Structure of Gravastar

Here, we explore the geometrical composition of gravastar with Kuchowicz metric function in $f(R, T)$ scenario. We inspect the regions of gravastar, i.e., (1) the inner, (2) the intermediate thin-shell and (3) the outer. The internal domain of gravastar is enclosed by thin-shell which consists of stiff matter while the outer domain is entirely a vacuum and the Schwarzschild spacetime can be identified suitable for this external system. The shell is assumed to be extremely thin having a finite width satisfying the range $\mathcal{R}_1 = \mathcal{R} < r < \mathcal{R} + \epsilon = \mathcal{R}_2$, in which \mathcal{R}_1 and \mathcal{R}_2 indicate the interior and exterior radii of gravastar, respectively and thickness of the shell is exhibited by $\mathcal{R}_2 - \mathcal{R}_1 = \epsilon$. Thus, the composition of gravastar can be specified by three geometries based on the following EoS

- Internal geometry (\mathcal{G}_1) $\Rightarrow p + \rho = 0$ for $0 \leq r < \mathcal{R}_1$,
- Thin-shell (\mathcal{G}_2) $\Rightarrow p = \rho$ for $\mathcal{R}_1 \leq r \leq \mathcal{R}_2$,
- External geometry (\mathcal{G}_3) $\Rightarrow p = \rho = 0$ for $\mathcal{R}_2 < r$.

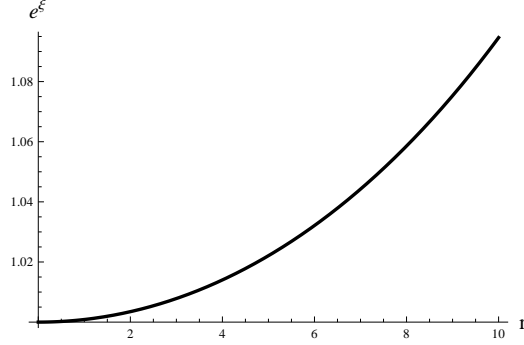


Figure 1: Plot of $e^{\xi(r)}$ against $r(km)$ with $\alpha = 0.2$ and $\rho_c = 0.0001$.

3.1.1 The Inner Geometry

In this domain, following the concept of Mazur and Mottola [1], we take the EoS $\mathcal{W}\rho = p$ with \mathcal{W} being the parameter of EoS and on setting $\mathcal{W} = -1$, we obtain $-\rho = p$ which manifests the dark energy EoS. The negative pressure in this EoS acts radially outward from the core of spherical object to overcome the inward directed pull by the thin-shell. Hence, the dark energy is responsible for this repulsive force in the inner domain of gravastar. With the help of this EoS, Eq.(18) yields $\rho = \rho_c(\text{constant})$, and hence

$$p = -\rho = -\rho_c. \quad (19)$$

This equation demonstrates that throughout the interior geometry, the pressure and matter density remain constant. Inserting this equation in Eq.(15), the other metric function $e^{\xi(r)}$ is obtained as

$$e^{-\xi(r)} = 1 - \frac{4(\alpha + 2\pi)r^2\rho_c}{3} + \frac{C_1}{r}, \quad (20)$$

where C_1 is the integration constant and we put $C_1 = 0$ to obtain the regular solution at the center, i.e., $r = 0$. Consequently, Eq.(20) becomes

$$e^{-\xi(r)} = 1 - \frac{4(\alpha + 2\pi)r^2\rho_c}{3}. \quad (21)$$

The analysis of $e^{\xi(r)}$ against radial component is presented in Figure 1 for particular values of α and ρ_c which interprets that this metric function is

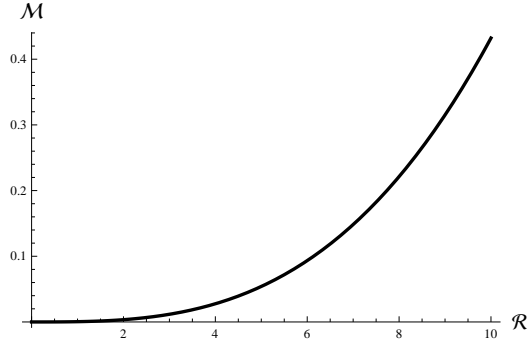


Figure 2: Evolution of gravitational mass (M_{\odot}) versus $\mathcal{R}(km)$ with $\alpha = 0.2$ and $\rho_c = 0.0001$.

singularity free as well as regular inside the gravastar. In the interior geometry, the active gravitational mass can be evaluated through the following equation

$$\mathcal{M}(\mathcal{R}) = 4\pi \int_0^{\mathcal{R}_1=\mathcal{R}} r^2 \left[\rho - \frac{\alpha}{8\pi} (p - 3\rho) \right] dr = \frac{2(2\pi + \alpha)\mathcal{R}^3 \rho_c}{3}. \quad (22)$$

The behavior of gravitational mass is displayed in Figure 2 which shows that the metric is free from any singularity at the center of gravastar.

3.1.2 The Intermediate Shell

Here, we assume that the intermediate gravastar thin-shell consists of stiff/ultra-relativistic matter obeying the EoS $p = \rho$. In connection with the cold baryonic universe, Zel'dovich [38] introduced the idea of such sort of matter distribution specified as stiff fluid configuration. In this scenario, it may arise due to the gravitational quanta at negligible temperature or because of some thermal perturbations with null chemical potential [1]. This fluid has been utilized by several researchers [39]-[43] to resolve different astrophysical as well as cosmological problems. Implementation of stiff fluid EoS in Eqs.(15) and (16) leads to

$$e^{-\xi(r)} = \frac{e^{Ar^2} - AC_2}{Ar^2 e^{Ar^2}}, \quad (23)$$

where the integration constant is presented by C_2 which may be evaluated by utilizing the boundary condition. Substituting Eq.(23) along with the stiff

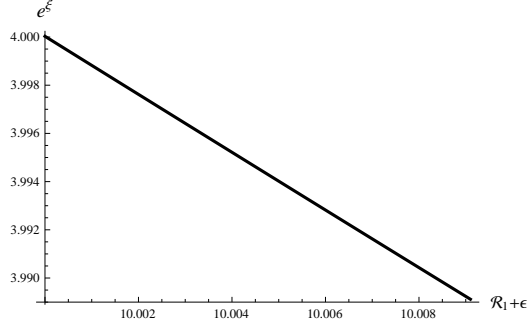


Figure 3: Variation of $e^{\xi(r)}$ versus thickness of the thin-shell.

fluid EoS and Kuchowicz metric function in Eq.(17), the matter density and pressure turn out to be

$$p = \rho = -\frac{1 - AC_2e^{-Ar^2} - Ar^2 - A^2r^4}{2(4\pi + \alpha)Ar^4}. \quad (24)$$

3.1.3 The Exterior Geometry and Boundary Conditions

It is well-known that the Einstein field equations are highly nonlinear in nature but possess one most significant solution outside the spherical object of total mass M , known as the Schwarzschild solution. The exterior geometry of gravastar satisfying the $\rho = p = 0$ EoS can be characterized by the Schwarzschild metric given by

$$ds_+^2 = \left(1 - \frac{2M}{r}\right) dt^2 - \frac{dr^2}{\left(1 - \frac{2M}{r}\right)} - r^2 d\theta^2 - r^2 \sin^2 \theta d\phi^2. \quad (25)$$

The structure of gravastar has two boundaries, one interrelates the internal geometry and intermediate thin-shell while the other connects the thin-shell and the external metric. For a viable system, the metric potentials should be continuous at these boundaries. In order to obtain the values of unknown constants A , B and C_2 , we match the metric potentials at the interfaces as follows

$$A = \frac{-M}{\mathcal{R}_2^2(2M - \mathcal{R}_2)}, \quad (26)$$

$$B = \sqrt{\left(1 - \frac{2M}{\mathcal{R}_2}\right) e^{\frac{M}{2M - \mathcal{R}_2}}}, \quad (27)$$

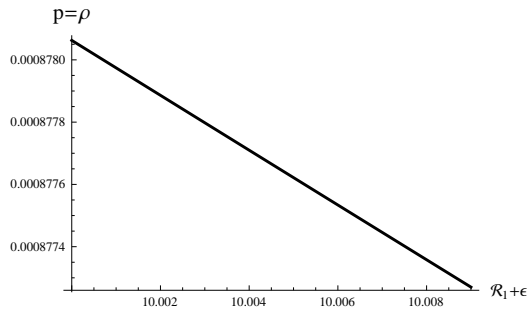


Figure 4: Behavior of $p = \rho$ (km^{-2}) versus thickness with $\alpha = 0.2$.

$$C_2 = \frac{e^{A\mathcal{R}_2^2}}{A} - \mathcal{R}_2^2 e^{A\mathcal{R}_2^2} \left(1 - \frac{2M}{\mathcal{R}_2}\right). \quad (28)$$

To determine the values of these constants, we consider mass of the gravastar $M = 3.75M_\odot$, inner radius $\mathcal{R}_1 = 10km$ and outer radius $\mathcal{R}_2 = 10.009km$ [44] which provide $A = 0.01491932683km^{-2}$, $B = 0.2371387429$ and $C_2 = 186.8400519$. The evolution of the metric potential (23) as well as the matter density and pressure (24) by inserting the above calculated values of unknowns are displayed in Figures 3 and 4, respectively. We see that the metric function does not possess any singularity and pressure or energy density exhibits positive values throughout the thin-shell of gravastar which sharply decrease with thickness of the shell.

3.1.4 Darmois-Israel Matching Constraint

The study of astrophysical objects demands that there must be a smooth connection between inner and outer geometries. We have already discussed that the structure of gravastar depends upon three domains, i.e., \mathcal{G}_1 , \mathcal{G}_2 and \mathcal{G}_3 in which \mathcal{G}_2 acts as a junction between \mathcal{G}_1 and \mathcal{G}_3 . Implementing the Darmois-Israel formalism [45, 46], there must be a smooth relation between \mathcal{G}_1 and \mathcal{G}_3 geometries of the gravastar. At the junction ($r = \mathcal{R}$), though the coefficients of the metric are continuous but their differentials may not be continuous at this interface. In order to evaluate the stress-energy of the surface (\mathcal{S}_{ab}), we consider the Lanczos equation [47, 48] expressed by

$$\mathcal{S}_b^a = \frac{1}{8\pi} (\alpha_b^a \mu_\lambda^\lambda - \mu_b^a), \quad (29)$$

where $\mu_{ab} = \mathcal{K}_{ab}^+ - \mathcal{K}_{ab}^-$ yields the discontinuous form of the extrinsic curvature. Here, the $-$ and $+$ signs manifest the inner and outer domains of gravastar, respectively.

The extrinsic curvature along with two regions of the intermediate shell is characterized by

$$\mathcal{K}_{ab}^\pm = -\Upsilon_\nu^\pm \left[\frac{\partial^2 x^\nu}{\partial \zeta^a \partial \zeta^b} + \Gamma_{\alpha\beta}^\nu \frac{\partial x^\alpha \partial x^\beta}{\partial \zeta^a \partial \zeta^b} \right], \quad (30)$$

where ζ^a symbolizes the intrinsic coordinates on the thin-shell while Υ_ν^\pm reveal the unit normals at hypersurface. For the line element

$$ds^2 = \mathcal{J}(r)dt^2 - \frac{dr^2}{\mathcal{J}(r)} - r^2 d\theta^2 - r^2 \sin^2 \theta d\phi^2, \quad (31)$$

the unit normals are described as

$$\Upsilon_\nu^\pm = \pm \left| g^{\alpha\beta} \frac{\partial \mathcal{J}}{\partial x^\alpha} \frac{\partial \mathcal{J}}{\partial x^\beta} \right|^{-\frac{1}{2}} \frac{\partial \mathcal{J}}{\partial x^\nu}, \quad \text{satisfying} \quad \Upsilon^\nu \Upsilon_\nu = 1. \quad (32)$$

Adopting the Lanczos equations, the mathematical expression of $\mathcal{S}_{ab} = \text{diag}(\Omega, -\mathcal{P}, -\mathcal{P}, -\mathcal{P})$ is acquired with Ω being the surface energy density and \mathcal{P} being the surface pressure. The forms of Ω and \mathcal{P} are demonstrated by

$$\Omega = -\frac{1}{4\pi\mathcal{R}} \left[\sqrt{\mathcal{J}} \right]_-^+, \quad \mathcal{P} = \frac{-\Omega}{2} + \left[\frac{\mathcal{J}'}{16\pi\sqrt{\mathcal{J}}} \right]_-^+. \quad (33)$$

Inserting \mathcal{G}_1 and \mathcal{G}_3 geometries of gravastar in the above forms, we obtain

$$\Omega = \frac{1}{4\pi\mathcal{R}} \left[\sqrt{1 - \frac{4(2\pi + \alpha)\mathcal{R}^2 \rho_c}{3}} - \sqrt{1 - \frac{2M}{\mathcal{R}}} \right], \quad (34)$$

$$\mathcal{P} = -\frac{1}{8\pi\mathcal{R}} \left[\frac{1 - \frac{8(2\pi + \alpha)\mathcal{R}^2 \rho_c}{3}}{\sqrt{1 - \frac{4(2\pi + \alpha)\mathcal{R}^2 \rho_c}{3}}} - \frac{1 - \frac{M}{\mathcal{R}}}{\sqrt{1 - \frac{2M}{\mathcal{R}}}} \right]. \quad (35)$$

The graphical description of Ω and \mathcal{P} is exhibited in Figure 5. It is found that both the parameters display finite as well as positive behavior within the shell which assures the creation and stability of the intermediate thin-shell of gravastar. Employing Eq.(34), we derive the surface mass for the thin-shell of gravastar as

$$\mathcal{M}_{shell} = 4\pi\mathcal{R}^2\Omega = \mathcal{R} \left[\sqrt{1 - \frac{4(2\pi + \alpha)\mathcal{R}^2 \rho_c}{3}} - \sqrt{1 - \frac{2M}{\mathcal{R}}} \right], \quad (36)$$

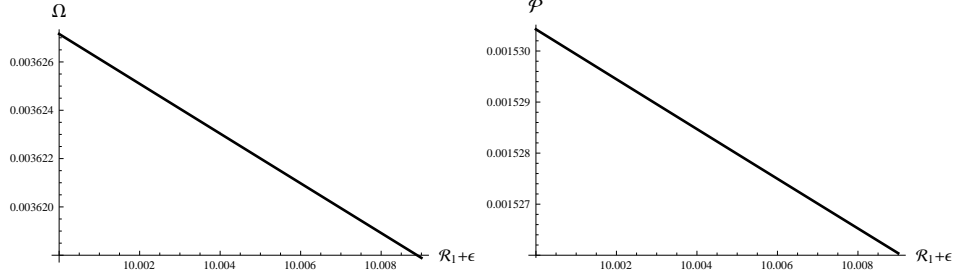


Figure 5: Variation of Ω and \mathcal{P} versus thickness of thin-shell with $\alpha = 0.2$ and $\rho_c = 0.0001$.

which provides the total mass in the form of mass of gravastar thin-shell as follows

$$M = \frac{2(2\pi + \alpha)\mathcal{R}^3\rho_c}{3} - \frac{\mathcal{M}_{shell}^2}{2\mathcal{R}} + \mathcal{M}_{shell}\sqrt{1 - \frac{4(2\pi + \alpha)\mathcal{R}^2\rho_c}{3}}. \quad (37)$$

4 Some Features of Gravastar Shell

This section inspects some necessary features of gravastar like EoS parameter, proper length, energy-thickness relationship and surface redshift that completely portray the intermediate thin-shell of gravastar.

4.1 The EoS Parameter

For the intermediate geometry of gravastar, Eqs.(34) and (35) lead to the parameter of EoS at $r = \mathcal{R}$ as

$$\mathcal{W}(\mathcal{R}) = \frac{\mathcal{P}}{\Omega} = \frac{\left[\frac{1 - \frac{8(2\pi + \alpha)\mathcal{R}^2\rho_c}{3}}{\sqrt{1 - \frac{4(2\pi + \alpha)\mathcal{R}^2\rho_c}{3}}} - \frac{1 - \frac{M}{\mathcal{R}}}{\sqrt{1 - \frac{2M}{\mathcal{R}}}} \right]}{2 \left[\sqrt{1 - \frac{2M}{\mathcal{R}}} - \sqrt{1 - \frac{4(2\pi + \alpha)\mathcal{R}^2\rho_c}{3}} \right]}. \quad (38)$$

The positive matter density and pressure always provide positive value of \mathcal{W} . For EoS parameter to be real, the required constraints are $\frac{2M}{\mathcal{R}} < 1$ and $\frac{4(2\pi + \alpha)\mathcal{R}^2\rho_c}{3} < 1$. Further, by expanding the square-root terms both in the

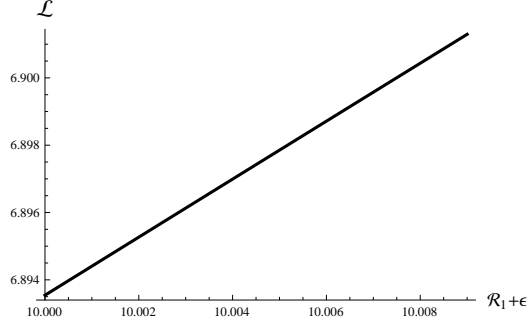


Figure 6: Variation of \mathcal{L} (km) versus thickness of thin-shell.

denominator as well as numerator of Eq.(38) in a binomial series along with the constraints $\frac{M}{\mathcal{R}} \ll 1$ and $\frac{4(2\pi+\alpha)\mathcal{R}^2\rho_c}{3} \ll 1$ and considering the terms up to first order, we can attain

$$\mathcal{W}(\mathcal{R}) \approx \frac{3}{2\left[\frac{3M}{2(\alpha+2\pi)\mathcal{R}^3\rho_c} - 1\right]}. \quad (39)$$

From this expression, the two possibilities for $\mathcal{W}(\mathcal{R})$ can clearly be examined, i.e., $\mathcal{W}(\mathcal{R})$ is either negative if $\frac{2(\alpha+2\pi)\rho_c}{3} > \frac{M}{\mathcal{R}^3}$, or $\mathcal{W}(\mathcal{R})$ is positive if $\frac{2(\alpha+2\pi)\rho_c}{3} < \frac{M}{\mathcal{R}^3}$.

4.2 Proper Length for Intermediate Shell

It has been assumed that the domain of stiff fluid gravastar shell is situated at the boundary $r = \mathcal{R}$ which is specified through the geometry \mathcal{G}_1 . As, the thin-shell is considered to be comprised of very small thickness, i.e., $\epsilon \ll 1$, therefore, the geometry \mathcal{G}_3 originates from the surface $r = \mathcal{R} + \epsilon$. Hence the proper length (\mathcal{L}) of the thin-shell is determined by the expression

$$\mathcal{L} = \int_{\mathcal{R}}^{\mathcal{R}+\epsilon} \sqrt{e^{\xi(r)}} dr = \left[\frac{\ln \left\{ e^{\frac{Ar^2}{2}} + \sqrt{e^{Ar^2} - AC_2} \right\}}{\sqrt{Ae^{\frac{Ar^2}{2}}}} \right]_{\mathcal{R}}^{\mathcal{R}+\epsilon}. \quad (40)$$

The graphical behavior of the proper length with respect to the thickness of thin-shell gravastar is displayed in Figure 6 which manifests the linear as well as increasing relation between them.

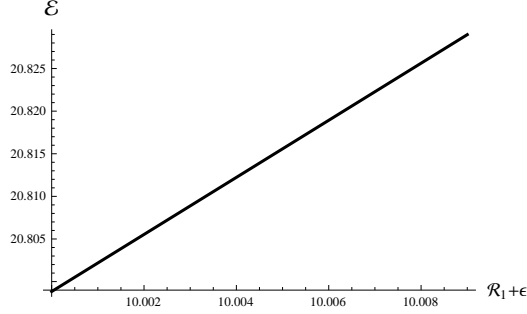


Figure 7: Evolution of energy (km) versus thickness (km) with $\alpha = 0.2$.

4.3 Energy within the Thin-Shell

In the geometry \mathcal{G}_1 , we have adopted the dark energy EoS which expresses the negative matter density yielding the presence of repulsive effects in the inner geometry of gravastar. In $f(R, T)$ framework, the expression of energy in the intermediate shell of gravastar turns out to be

$$\mathcal{E} = 4\pi \int_{\mathcal{R}}^{\mathcal{R}+\epsilon} \rho r^2 dr = \frac{-4\pi}{4\pi + \alpha} \int_{\mathcal{R}}^{\mathcal{R}+\epsilon} \left[\frac{1 - Ar^2 - A^2 r^4 - AC_2 e^{-Ar^2}}{2Ar^2} \right] dr,$$

whose integration leads to

$$\mathcal{E} = \frac{-4\pi}{4\pi + \alpha} \left[\frac{C_2 e^{-Ar^2}}{r} - \frac{1}{Ar} - \frac{2Ar^3}{3} - r + \sqrt{AC_2\pi} \text{Erf}[\sqrt{Ar}] \right]_{\mathcal{R}}^{\mathcal{R}+\epsilon}, \quad (41)$$

where Erf stands for the error function. The graphical analysis of energy versus thickness demonstrates the attractive nature of energy within the thin-shell and is shown in Figure 7.

4.4 Surface Redshift within the Thin-Shell

In the study of structure of gravastars, the surface redshift can be regarded as one of the most significant sources of information corresponding to the detection as well as stability of gravastars. For static isotropic matter distribution, it is claimed that the value of redshift parameter should not exceed 2 [49, 50]. The expression of surface redshift is presented by [34]

$$\mathcal{Z}_s = |g_{tt}|^{\frac{-1}{2}} - 1 = \frac{1}{e^{\frac{Ar^2}{2}} B} - 1. \quad (42)$$

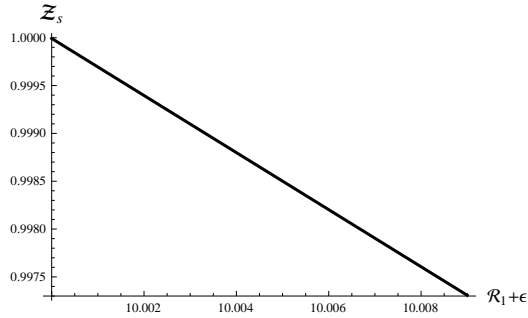


Figure 8: Behavior of \mathcal{Z}_s against thickness of thin-shell.

The behavior of surface redshift (by substituting the numerical values of A and B) is exhibited in Figure 8 which indicates that the value of redshift parameter lies within 1 inside the intermediate thin-shell of gravastar. Hence, we can claim the stable as well as physically consistent structure of gravastar.

5 Concluding Remarks

In this work, we have evaluated a new solution to study a novel massive compact object named as gravastar in $f(R, T)$ framework by considering the Kuchowicz metric function. This massive stellar model can be regarded as a feasible substitute for a black hole. The motivation behind the consideration of Kuchowicz metric potential is that this metric function is purely non-singular and exhibits a regular behavior within the geometry of gravastar. We have discussed various properties of three geometries of gravastar with respect to $R + 2\alpha T$ functional form. We have obtained regular solutions for the interior geometry at the center of gravastar and analyzed different characteristics of the thin-shell for a particular value of α which leads to physical viability of the gravastar.

In the interior geometry of gravastar, we have acquired solution of the metric potential, matter density and pressure. Using the dark energy EoS in the conservation equation, we have determined that the matter density remains constant throughout the inner region. This constant value of density is responsible for the outward pull to keep the gravastar in stable state. The evolution of the metric function $e^{\xi(r)}$ (Figure 1) remains finite at the core of interior geometry. The behavior of gravitational mass has also been analyzed

which becomes zero at the origin and positive within the interior domain. Thus, the considered metric avoids any type of central singularity.

In the intermediate thin-shell of gravastar, we have assumed the ultra-relativistic matter configuration and solved the field equations to evaluate the metric function. For the exterior geometry, we have employed the Schwarzschild metric and calculated the values of unknown constants through boundary conditions. We have also determined the surface density and pressure by utilizing the Darmois-Israel matching constraints. We have then inspected some important aspects of gravastar like variation of matter density or pressure, EoS parameter, proper length, energy and surface redshift associated with the thickness of the thin-shell. All these parameters manifest the stable structure of gravastar and demonstrate the physical acceptability of our considered metric function as well as $f(R, T)$ model.

The exact solutions of the field equations play a crucial role to discuss the composition of astrophysical objects. Das et al. [29] presented different features of gravastar in $f(R, T)$ framework and evaluated a set of complete solutions for three different regions with their corresponding EoS. Shamir and Ahmad [30] solved the $f(\mathcal{G}, T)$ field equations to obtain non-singular solutions of gravastar. Yousaf et al. [51] observed the effects of electromagnetic field on the formation of gravastar for $R + 2\chi T$ model of $f(R, T)$ gravity. Yousaf and his collaborators [52] discussed the significance and characteristics of gravastar under some specific constraints in $f(R, T, R_{\mu\nu}T^{\mu\nu})$ gravity. Bhatti et al. [53] explored the non-singular spherical model with a particular EoS in $f(R, G)$ gravity. In all these works, the authors have not used any particular metric potential to inspect physically viable structure of gravastar in modified theories.

In the context of GR, Ghosh et al. [34] investigated the regions of gravastar by adopting the Kuchowicz metric potential. They analyzed various features of gravastar graphically and found stable structure under the effect of their considered non-singular metric potential. We have obtained new exact solutions of $f(R, T)$ field equations by implementing Kuchowicz metric potential to describe the geometries of gravastar. We conclude that the construction of gravastar like stellar model admitting the Kuchowicz metric potential in this framework seems to be physically consistent as well as viable similar to GR [34]. Hence, $f(R, T)$ gravity can provide stable as well as acceptable structures of massive compact objects under the influence of specific metric function same as in GR. It would be interesting to discuss different regions of gravastar with respect to several other types of metric functions

in $f(R, T)$ theory as well as in other modified gravitational theories.

References

- [1] Mazur, P. and Mottola, E.: Proc. Natl. Acad. Sci. USA **101**(2004)9545.
- [2] Chapline, G. et al.: Int. J. Mod. Phys. A **18**(2003)3587.
- [3] Lobo, F.S.N.: Class. Quantum Grav. **23**(2006)1525.
- [4] Chirenti, C.B.M.H. and Rezzolla, L. Phys. Rev. D **78**(2008)084011.
- [5] Visser, M. and Wiltshire, D.L.: Class. Quantum Grav. **21**(2004)1135.
- [6] Carter, B.M.N.: Class. Quantum Grav. **22**(2005)4551.
- [7] Bilić, N., Tupper, G.B. and Viollier, R.D.: J. Cosmol. Astropart. Phys. **02**(2006)013.
- [8] Horvat, D. and Ilijić, S.: Class. Quantum Grav. **24**(2007)5637.
- [9] Broderick, A.E. and Narayan, R.: Class. Quantum Grav. **24**(2007)659.
- [10] Chirenti, C.B.M.H. and Rezzolla, L. Class. Quantum Grav. **24**(2007)4191.
- [11] Rocha, P. et al.: J. Cosmol. Astropart. Phys. **11**(2008)010.
- [12] Cardoso, V. et al.: Phys. Rev. D **77**(2008)124044.
- [13] Harko, T., Kovács, Z. and Lobo, F.S.N.: Class. Quantum Grav. **26**(2009)215006.
- [14] Pani, P. et al.: Phys. Rev. D **80**(2009)124047.
- [15] Lobo, F.S.N. and Arellano, A.V.B.: Class. Quantum Grav. **24**(2007)1069.
- [16] Horvat, D., Ilijić, S. and Marunovic, A.: Class. Quantum Grav. **26**(2009)025003.
- [17] Turimov, B.V., Ahmedov, B.J. and Abdujabbarov, A.A.: Mod. Phys. Lett. A **24**(2009)733.

- [18] Harko, T. et al.: Phys. Rev. D **84**(2011)024020.
- [19] Haghani, Z. et al.: Phys. Rev. D **88**(2013)044023; Odintsov, S.D. and Sáez-Gómez, D.: Phys. Lett. B **725**(2013)437.
- [20] Sharif, M. and Ikram, A.: Eur. Phys. J. C **76**(2016)640.
- [21] Moraes, P.H.R.S., Arbañil, J.D.V. and Malheiro, M.: J. Cosmol. Astropart. Phys. **06**(2016)005.
- [22] Sharif, M. and Siddiqa, A.: Eur. Phys. J. Plus **132**(2017)529.
- [23] Das, A.: Phys. Rev. D **95**(2017)124011.
- [24] Sharif, M. and Waseem, A.: Gen. Relativ. Gravit. **50**(2018)78.
- [25] Deb, D. et al.: J. Cosmol. Astropart. Phys. **03**(2018)044.
- [26] Sharif, M. and Waseem, A.: Eur. Phys. J. C **50**(2018)78.
- [27] Sharif, M. and Siddiqa, A.: Int. J. Mod. Phys. D **27**(2018)1850065; Ad. High Energy Phys. **2019**(2019)8702795.
- [28] Sharif, M. and Waseem, A.: Int. J. Mod. Phys. D **28**(2019)1950033; 2040005.
- [29] Das, A. et al.: Phys. Rev. D **95**(2017)124011.
- [30] Shamir, F. and Ahmad, M.: Phys. Rev. D **97**(2018)104031.
- [31] Cattoen, C., Faber, T. and Visser, M.: Class. Quantum Grav. **22**(2005)4189.
- [32] DeBenedictis, A. et al.: Class. Quantum Grav. **23**(2006)2303.
- [33] Chan, R., da Silva, M.F.A. and Rocha, P.: Gen. Relativ. Gravit. **43**(2011)2223.
- [34] Ghosh, S. et al.: Res. Phys. **14**(2019)102473.
- [35] Sharif, M. and Waseem, A.: Astrophys. Space Sci. **364**(2019)189.
- [36] Ghosh, S. et al.: Ann. Phys. **411**(2019)167968.

- [37] Kuchowicz, B.: Acta. Phys. Pol. **33**(1968)541.
- [38] Zel'dovich, Y.B.: Mon. Not. R. Astron. Soc. **160**(1972)1.
- [39] Carr, B.J.: Astrophys. J. **201**(1975)1.
- [40] Wesson, P.S.: J. Math. Phys. **19**(1978)2283.
- [41] Madsen, M.S. et al.: Phys. Rev. D **46**(1992)1399.
- [42] Braje, T.M. and Romani, R.W.: Astrophys. J. **580**(2002)1043.
- [43] Linares, L.P., Malheiro, M. and Ray, S.: Int. J. Mod. Phys. D **13**(2004)1355.
- [44] Ghosh, S., Ray, S., Rahaman, F. and Guha, B.K.: Ann. Phys. **394**(2018)230.
- [45] Darmois, G. *Mémoire des sciences mathématiques XXV, Fascicule XXV* (Gauthier-Villars, Paris, France, 1927).
- [46] Israel, W.: Nuovo Cimento B **44**(1966)1.
- [47] Lanczos, K.: Ann. Phys. (Berlin) **379**(1924)518.
- [48] Sen, N.: Ann. Phys. (Leipzig) **378**(1924)365.
- [49] Buchdahl, H.A.: Phys. Rev. **116**(1959)1027.
- [50] Barraco, D.E. and Hamity, V.H.: Phys. Rev. D **65**(2002)124028.
- [51] Yousaf, Z., Bamba, K., Bhatti, M.Z. and Ghafoor, U.: Phys. Rev. D **100**(2019)024062.
- [52] Yousaf, Z., Bhatti, M.Z. and Asad, H.: Phys. Dark Univ. **28**(2020)100527.
- [53] Bhatti, M.Z., Yousaf, Z. and Rehman, A.: Phys. Dark Univ. **29**(2020)100561.